



Groundwater recharge mechanisms in a vegetated epikarst spring catchment using water isotopes methods

Yan Deng¹ · Aijun Zhu³ · Yanqing Li¹ · Fen Yi² · Qinjun Zhang⁴ · Jing Ke²

Accepted: 19 December 2022 / Published online: 4 January 2023

© The Author(s), under exclusive licence to Springer-Verlag GmbH Germany, part of Springer Nature 2023

Abstract

Estimating groundwater recharge mechanisms is essential for sustainable and effective groundwater management. Groundwater recharge and evapotranspiration quantification is a key step to properly manage and protect valuable groundwater resources. For this study, precipitation and throughfall (the essential recharge elements of epikarst zones) were evaluated to separately calculate evaporation, groundwater recharge, and groundwater residence times (MRT) in a forested epikarst spring catchment. The d-excess and water balance methods were employed to quantify evaporation and transpiration in a spring catchment. The results revealed that 72.1% of summer precipitation and 27.9% of winter precipitation contributed to the recharge of epikarst spring water. The durations from precipitation to spring discharge using the $\delta^{18}\text{O}$ method (121 days) were a little shorter than that from throughfall to spring discharge. The calculated results using d-excess in a forested catchment were 3.16% for the total evaporation. The ratios of transpiration to evapotranspiration in the vegetated catchment were 51.22%, indicating that the main water consumption in vegetated watersheds was vegetation transpiration. The d-excess method provided new insights into the quantifications of the components of the water circulation.

Keywords Evaporation rate · Groundwater recharge · Groundwater residence times · Deuterium excess · Epikarst spring catchment

Introduction

Karst groundwater is an important water resource for humans, as about 25% of the global population completely or partially relies on drinking water from karst aquifers (Hartmann et al. 2014). Sustainable and effective management of groundwater resources requires a systematic and comprehensive understanding of groundwater recharge mechanisms to assess any changes in water budget affected by deforestation and climate change (Tayoko and Yoshio 2004). So, the study of groundwater recharge mechanism,

including estimating the recharge rate, average residence time and segregating watershed evapotranspiration by evaporation and transpiration, is essential to predict a lot of the contribution to groundwater resources and their available socio-economic development.

Karst region is characterized by an extremely heterogeneous porosity, such as micropores, fissures, and conduits (Ford and Williams 2007; Hartmann et al. 2014; Gholam et al. 2016), which lead to a strong heterogeneity of the water flow at the ground and in the underground (Hartmann et al. 2014). Vegetation impact infiltration rate and flow change the recharge form of rainfall to epikarst zone (Allen et al. 2014; Hiroaki et al. 2013; Deng et al. 2019). Groundwater recharge mechanisms and rates in a forested epikarst spring catchment depend on underlying surface conditions (geology, geomorphology, rock exposure rate, soil distribution and thickness, etc.), plant physiological characteristics (plant species and growth process, etc.) and meteorological factors (rainfall, photosynthetic effective radiation, vapor pressure deficit, and wind speed, etc.) (Deng et al. 2019; Martin et al. 2020). Previous studies on groundwater recharge mechanism mainly focused on karst water process in different watershed

✉ Yan Deng
dydesk@163.com

¹ College of Environment and Resources, Guangxi Normal University, Guilin 541004, China

² Institute of Karst Geology, Chinese Academic of Geological Sciences, Guilin 541004, China

³ School of Electronic Engineering and Automation, Guilin University of Electronic Technology, Guilin 541004, China

⁴ Guangxi Geological Survey Institute, Nanning 530023, China

(Fu et al. 2016; Reddy et al. 2006), ground-water recharge (Mohamed et al. 2021; Ahmet et al. 2020; Gholam et al. 2016) and karst water resources assessment (Lee et al. 2007; Hartmann et al. 2014).

Transpiration and evaporation are critical components of the water budget of forested catchments (Tayoko and Yoshio 2004; Hu et al. 2018). An important step in groundwater evaluations is to segment evapotranspiration by transpiration and evaporation. Recently, an increasing number of researchers have utilized hydrogen and oxygen isotopes to segregate watershed evapotranspiration by evaporation and transpiration, based on the Rayleigh equation (Maki and Tadashi 1998; Tayoko and Yoshio 2004; Liu et al. 2006; Hu et al. 2018). The evaporation to evapotranspiration ratio was estimated to be between 3 and 21.4%, by contrasting the differences between the initial isotopic content of groundwater and the final content at a catchment outlet (Maki and Tadashi 1998; Tayoko and Yoshio 2004; Liu et al. 2006; Hu et al. 2018). Furthermore, the empirically estimated d-excess values ($d\text{-excess} = \delta D - 8 \times \delta^{18}O$) (Dansgaard 1964), were also employed to estimate evaporation in watersheds (Huang and Pang 2012; Hu et al. 2018) based on its sensibility of non-equilibrium fractionation processes and the different diffusivities of water stable isotope during the evaporation and transpiration (Mauro et al. 2020). To improve the evaluation of groundwater process and water budgets, groundwater source, residence times, and evapotranspiration should be evaluated systematically.

The main objectives of this study were to estimate groundwater recharge source and groundwater residence times using stable water isotopes to segment evaporation and transpiration components by d-excess and water balance

methods in a forested epikarst spring catchment, Southwest China. Our research could provide new insights on the quantification of components of the water cycle. Furthermore, our results may assist in developing and managing groundwater resources more effectively and systematically in karst forest catchments.

Materials and methods

Study area

The study was conducted in a typical vegetated basin (S_{31} epikarst spring catchment), in Guilin, Guangxi, China (Fig. 1). Humid and subtropical monsoon dominates in this area with an annual average air temperature of 18.8 °C, average annual precipitation of 1915.2 mm, ~80% of which occurs during the rainy season (May to October) (Deng et al. 2020), and an average annual relative humidity of 76% to 82% (Zhu et al. 2017). The main lithology is thick limestone of the upper Devonian Rongxian Formation (D_{3r}) (Deng et al. 2020). The S_{31} epikarst spring catchment has an area of ~1 km² and consists of three flat depressions and 15 mountains with elevations of 400 and 652 m, which are dominated by karst peak-cluster depressions. The S_{31} spring is located at the bottom of a hill slope, which occurs off the junction between peak-cluster depression area and peak-forest plain, and flows from the epikarst zone through developed conduits. Preliminary findings showed that No.1 and No.4 depressions (Fig. 1) have good connectivity with No. S_{31} spring (Chang et al. 2012). The connectivity between No.3 depression and the S_{31} spring is poor, which may be

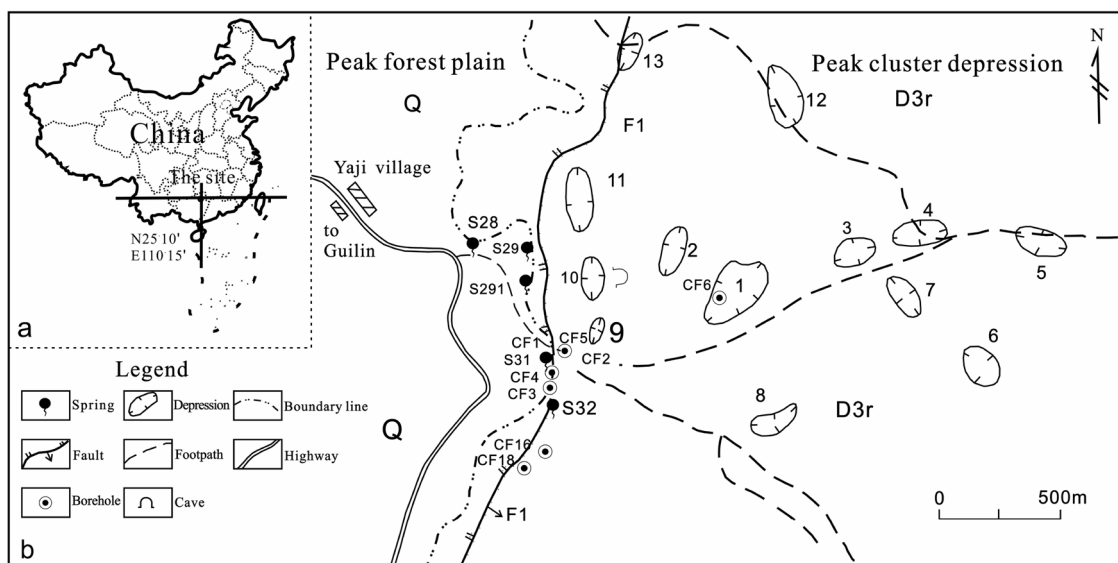


Fig. 1 Location of the study area in China (a) sketched hydrogeology map of the Yaji experimental station (b)

related to the lack of fracture development at the bottom of No.3 depression. During rainstorms, the surface runoff generated in the three depressions enters the karst conduit through a sinkhole at the bottom of the catchment (Chang et al. 2012). Based on borehole data, the thickness of epikarst zone ranges from ~8 to 10 m. The karst aquifers with coexisting conduits and cracks in the research areas have a high spatial heterogeneity, and the spring water is of the Ca-HCO₃ type. The discharge varies from 0 to 2.5 m³/s and quickly responds to precipitation (Chang et al. 2012). The catchment has a high limestone outcrop ratio, where soils are discontinuously distributed only within gaps. The average soil thickness is 5–10 cm with a maximum value of 100 cm in depressions. The soils are well drained, gravelly, and calcareous. This catchment experienced severe deforestation in the 1950s and has been under natural restoration for almost 70 years. Currently, natural shrubwood occupies ~77% of the total catchment area. *Caesalpinia decapetala* is the main species in the area, accompanied by *Toona sinensis*. *Caesalpinia decapetala* and *Toona sinensis* communities occupy 70% and 30% of the catchment, respectively.

Water sampling

Rainwater, throughfall and epikarst water following individual rain events from July 2015 to October 2016 were collected for H and O isotope analysis. Throughfall water sampling was conducted in two of the main vegetation (*Caesalpinia decapetala* and *Toona sinensis*) communities. Sixteen water collectors were positioned in a fixed, albeit random, pattern on each vegetated floor to collect throughfall. The rainwater from single precipitation events was collected via a funnel attached to a plastic tank, taking care to prevent evaporation. Spring water was collected while the throughfall water was collected. All water samples were stored in 15-mL capped plastic bottles, wrapped in para-film, and frozen pending stable isotope analysis.

Isotopic analyses

Stable isotopes of oxygen and hydrogen in the precipitation, throughfall, and epikarst spring water were measured using high-precision laser spectroscopy (LWIA-24d, Los Gatos Research, USA) at the Key Laboratory of Karst Dynamics, Institute of Karst Geology, at the Chinese Academy of Geological Science. The hydrogen and the oxygen isotope values are reported with respect to Vienna Standard Mean Ocean Water (VSMOW). The precision of the measurements was within ±0.1 ‰ for δ¹⁸O and ±0.3 ‰ for δ D.

The d-excess = δD – 8 × δ¹⁸O was calculated for all samples (Dansgaard, 1964). This index describes deviations from the meteoric water line (MWL) and can be used to

indicate the kinetic (i.e., no equilibrium) fractionation effects of evaporation (Gat 1996).

Seasonal groundwater recharge

Mass balance methods were employed to assess the proportional groundwater recharge contributions from summer and winter rainfall (Lee and Kim 2007). The distinct d-excess values of summer and winter rainfall were related to two end members for the respective seasons as,

$$d_{\text{excess-spring water}} = Xd_{\text{-Summer}} + (1 - X)d_{\text{-Winter}} \quad (1)$$

where *d*-excess was the deuterium excess value, *X* was the fraction of summer rainfall, and (1-*X*) was the fraction of winter rainfall.

Estimation of groundwater residence time

The groundwater residence time (MRT) in catchments was calculated by the seasonal isotopic fluctuation correlation between rainfall and epikarst spring water. The spring catchment was presumed to be mixed well and in a stable state, where MRT was assumed to have an exponential distribution (Reddy et al. 2006). The season isotopic fluctuation tended to a sine functional relationship as follow:

$$\delta = I + A \times \sin(ct - \theta) \quad (2)$$

where *I* was the annual average δD, δ¹⁸O, or d-excess in ‰, *A* was the seasonal amplitude of δD, δ¹⁸O, or d-excess, *c* was the fluctuation frequency of δD, δ¹⁸O, or d-excess, *t* was the time in days, *θ* was the phase lag in radians. The spring water MRT was calculated by the following formula:

$$\text{MRT} = C^{-1} \left[\left(\frac{A_{z2}}{A_{z1}} \right)^{-2} - 1 \right]^{0.5} \quad (3)$$

where *A*_{z1} was the seasonal amplitude of δ¹⁸O, δD, or d-excess of precipitation or throughfall, *A*_{z2} was the seasonal amplitude of δ¹⁸O, δD, or d-excess in epikarst water, and *C* was fluctuation frequency of δ¹⁸O, δD, or d-excess.

Estimating the evaporation rate in a vegetated area using the d-excess method

The evaporation rate in a vegetated catchment was calculated using the d-excess method including the dual water stable isotope (D-¹⁸O) (Hu et al. 2018). It was presumed that evaporation in a catchment experiences Rayleigh fractionation (Formula 4), where *R* was the ¹⁸O/¹⁶O or ²H/¹H ratio (Clark and Fritz 1997). For convenience, we employed an equation described by Hu et al. (2018), and *d* replaced *R*, thereby using δ to indicate the Rayleigh fractionation (formula 5). So, the relation between d-excess

and the spring water residual fraction was derived from formula 6. And 1-f was the evaporation ratio.

$$R = R_0 f^{(a-1)} \tag{4}$$

$$\delta = (\delta_0 + 1000) f^{(a-1)} - 1000 \tag{5}$$

$$d = \delta D - 8\delta^{18}O = (\delta D_0 + 1000) f^{(aD-1)} - 1000 - 8 \left[(\delta^{18}O_0 + 1000) f^{(a^{18}O-1)} - 1000 \right] = (\delta D_0 + 1000) f^{(aD-1)} - 8 (\delta^{18}O_0 + 1000) f^{(a^{18}O-1)} + 7000 \tag{6}$$

where *a* (the fractionation factor between the product and the reactant) was derived as in formula (7); α^* (the equilibrium fractionation factor) was obtained from formula (8) and (9). And ϵkD or ϵkO (the kinetic enrichment factor) was derived from formula (10) and (11). Furthermore, $\delta^{18}O_0$ and δD_0 were the initial groundwater isotopic content (here $\delta^{18}O_0$ or $\delta D_0 = \delta^{18}O_0$ or $\delta D_0 \times 1000$).

$$a = a_{\text{product}} - a_{\text{reactant}} = a_{v-1} = 1/(a^* + \epsilon k/1000) \tag{7}$$

$$\text{For } ^{18}O : \ln a^* = 1000 \times 1.137/T^2 - 0.4156/T - 2.0667/1000 \tag{8}$$

$$\text{For } D : \ln a^* = 1000 \times 24.844/T^2 - 76.248/T + 52.612/1000 \tag{9}$$

where the α^* for ^{18}O and for D (Hu et al. 2018) was given by the formula (8) and (9). Here, T was temperature (for T in K). Given an annual mean air temperature of 18.8 °C in the Yaji Basin, formula (8) yields a α^* value for ^{18}O of 1.010 and formula (9) yields a α^* value for D of 1.086.

$$\epsilon kD = 12.5(1 - h) \tag{10}$$

$$\epsilon kO = 14.2(1 - h) \tag{11}$$

$$ER = 1 - f \tag{12}$$

where *h* was the mean relative humidity given an annual mean air temperature of 80% in the Yaji Basin. ER is the evaporation ratio of the evapotranspiration rate in the catchment.

Chang et al. (2012) showed that the surface runoff only accounted for 0.63% of total discharge of S31 epikarst

spring. So, evapotranspiration ET in the study area was calculated through water balance method as follows:

$$ET = P - R \tag{13}$$

where *P* was precipitation and *R* was runoff. The evaporation ER (%) in basin was defined as:

$$ER = Ef/ET = (1 - f) \times TF/(P - R) \tag{14}$$

Here, the *P*, *R*, TF, δ , and δD were determined by ourselves in vegetated experimental catchment, and so the ER was calculated.

Results

Seasonal variations in precipitation, throughfall, and epikarst spring water

The annual mean values of the precipitation, throughfall, and spring flow in the epikarst spring catchment during the study period (July 2015–October 2016) are listed in Table 1. The annual weighted means of isotopic content in throughfall were -4.81‰ for $\delta^{18}O$ and -29.09‰ for δD , which are lower than those of precipitation. The isotope ratio of epikarst spring water was -6.20‰ in $\delta^{18}O$ and -38.65‰ in δD , which are also lower than those of precipitation and throughfall.

The relationships between $\delta^{18}O$ and δD compositions in precipitation, throughfall, and epikarst water are plotted in Fig. 2. A local meteoric water line (LMWL) at the S31 epikarst spring catchment was: $\delta D = 7.96\delta^{18}O + 8.67 (R^2 = 0.97; n = 92)$. Regression lines describing the isotopic data for different seasons were as follows: $\delta D = 8.04\delta^{18}O + 9.11 (R^2 = 0.96; n = 48)$ for the rainy season (from May to October), and $\delta D = 8.19\delta^{18}O + 15.96 (R^2 = 0.95; n = 18)$ for the dry season (November–April of the next year). The regression line in the epikarst spring water drawn through these data was: $\delta D = 8.40\delta^{18}O + 13.5 (R^2 = 0.95, n = 40)$, with $\delta D = 8.50\delta^{18}O + 14.15 (R^2 = 0.97, n = 29)$ for the rainy season (May–October), and $\delta D = -4.65\delta^{18}O - 73.98 (R^2 = 0.24, N = 11)$ for the dry season (November–April of the next year). The isotopes in the epikarst spring water were more stable than those in the precipitation and throughfall.

Table 1 Annual weighted mean water quantity, $\delta^{18}O$, δD , and d-excess of precipitation, throughfall and epikarst water (mean + SD)

Item	Water quantity(mm)	Runoff(L/S)	$\delta^{18}O$	δD	d-excess	<i>n</i>
Precipitation	15.91 ± 23.58	–	-4.79 ± 3.07	-28.16 ± 25.90	10.14 ± 5.50	94
Throughfalls	46.70 ± 32.47	–	-4.81 ± 3.20	-29.09 ± 26.69	9.41 ± 3.68	46
Epikarst water	–	51.48 ± 130.67	-6.20 ± 1.18	-38.65 ± 10.22	10.91 ± 2.38	47

n and SD were sample size and standard deviation

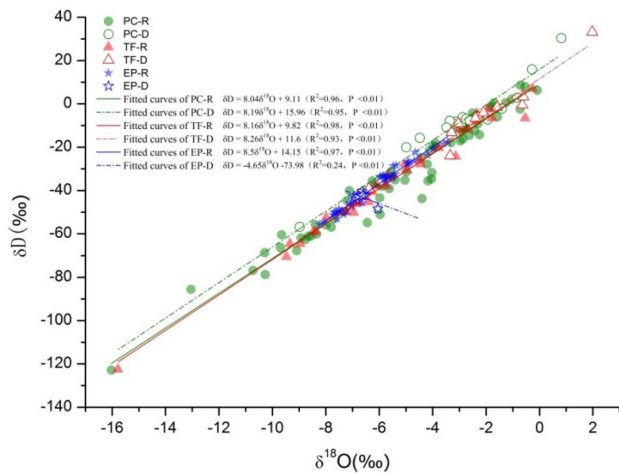


Fig. 2 Seasonal relation between contents of ^{18}O and D in precipitation, throughfall and epikarst spring water (PC was precipitation; TF was throughfall; EP was epikarst spring water; R was rainy season; D was dry season)

Seasonal variations in the water quantity and isotopes in precipitation, throughfall, and epikarst water are plotted in Fig. 3. The precipitation $\delta^{18}\text{O}$ was quite variable; however, the d-excess was stable, but $\delta^{18}\text{O}$ value changed greatly in the spring water.

Seasonal spring water recharge

Based on the mass balance formula (formula (1)), with end-member d-excess values of seasonal rainfall and epikarst spring water as input variables, the results indicated that 72.1% of the summer precipitation and 27.9% of the winter rainfall contributed to the spring water recharge. Although the study area was covered with dense vegetation, summer precipitation contributed more than that during winter, which suggested that the evapotranspiration effect was small in this area probably due to the rapid drainage of rainwater belowground through fissures and conduits.

Estimating MRT using $\delta\text{D}/\delta^{18}\text{O}$ methods

The isotopic content of precipitation, throughfall, and epikarst water was fitted, as shown in Fig. 4. The seasonal variation relationships of δD , $\delta^{18}\text{O}$, and d-excess between the precipitation or throughfall and groundwater during the hydrologic year were well mixed, and remained in a stable state in which MRT was assumed to approximate a sine regression (Fig. 4). Each curve had a good sine fitting relationship.

The groundwater MRTs of the vegetated catchment were calculated using formula (3) using $\delta\text{D}/\delta^{18}\text{O}$ and d-excess values and are presented in Table 2. Deuterium isotope has

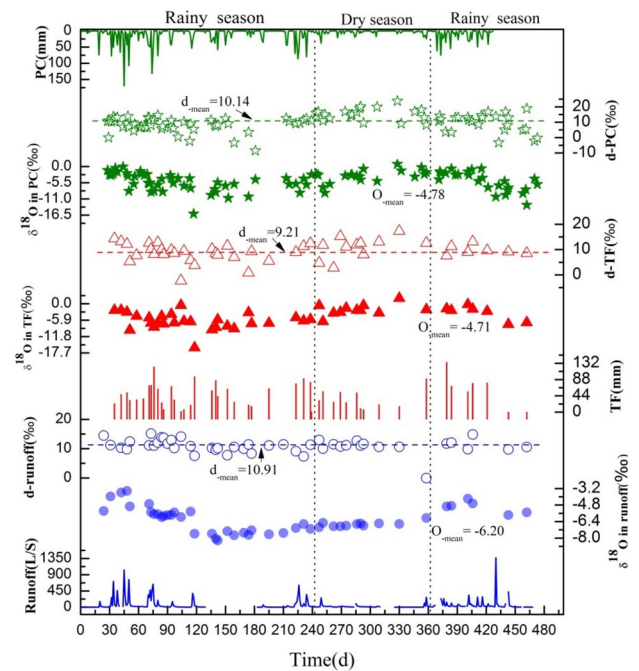


Fig. 3 Seasonal variations in water quantity and isotopes of precipitation, throughfall and epikarst water (PC was precipitation; TF was throughfall; dashed lines were the annual amount-weighted mean of d-excess)

a light mass, and hydrogen is eight times more affected by evaporation at the same temperature than that of oxygen. So, oxygen isotope is usually more stable than hydrogen isotope. The results of MRT calculated by oxygen isotope should be more reliable than that of hydrogen isotope and d-excess. Many studies also use oxygen isotope to calculate MRT (Maloszewski et al. 2002; Reddy et al. 2006; Rusjan et al 2019). Thus, the elapsed time from precipitation to spring discharge was 121 days using $\delta^{18}\text{O}$ values, and the durations from throughfall to spring discharge were 131 days using $\delta^{18}\text{O}$ values.

Estimation of evaporation rate using d-excess methods

The d-excess method was employed to estimate the evaporation amount, according to the isotopic content of precipitation and groundwater in a hydrological year. The data in Table 1 were used for the calculation. The evaporation proportion was calculated using formula (6). The calculated evaporation rates were 3.16% using the precipitation method (Table 3). The transpiration rate in the S_{31} epikarst spring catchment was 51.22% (Table 4) according to the water balances method and the evaporation calculated by the d-excess. Thus, the transpiration proportion in evapotranspiration was

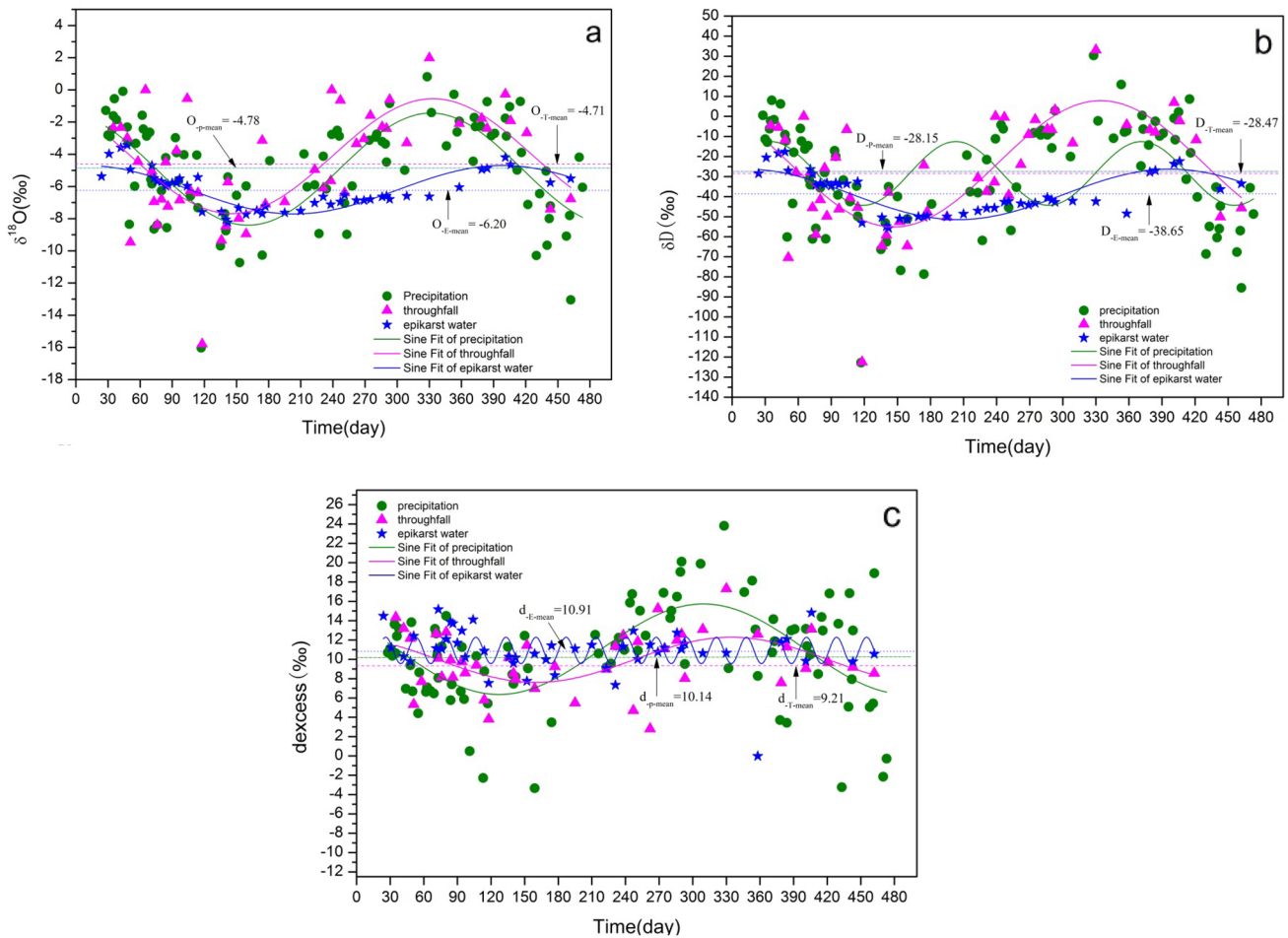


Fig. 4 Fitting curve of isotopes and d-excess (The dashed lines was the annual amount-weighted mean)

Table 2 The results of MRT

Item	Method	Amplitude of EP	Amplitude of PC or TF	C	MRT(days)
EP-PC	$\delta^{18}O$	1.51	3.49	0.017	120.98
	δD	12.57	15.92	0.027	28.96
	d-excess	1.36	4.68	0.126	26.19
TF-PC	$\delta^{18}O$	1.51	3.57	0.016	130.79
	δD	12.57	31.49	0.017	138.89
	d-excess	1.36	2.33	0.126	11.05

*EP is epikarst spring water, PC is precipitation, TF is throughfall

94.19%, which indicates that the catchment water cycle was dominated primarily by vegetation transpiration.

Discussion

Assessment of groundwater recharges ratio and groundwater renewal capacity

Karst acquirers are characterized by special hydrogeological conditions related to the dual media of fractures and conduits. Dispersed and centralized recharges are the two main

Table 3 δD , $\delta^{18}O$, and d-excess of spring water and the evaporation proportion (ER) by the d-excess method

Item	T	h	$\delta D_0(‰)$	$\delta^{18}O_0(‰)$	d_0 -excess(‰)	$\delta D(‰)$	$\delta^{18}O(‰)$	d-excess(‰)	ER(%)
PC method	18.8	0.8	-38.87	-6.21	10.91	-28.43	-4.83	10.14	3.16

*PC was precipitation

Table 4 Transpiration for the S31 epikarst spring catchment

Item	Water balance method			d-excess method			
	Precipitation (mm)	Runoff depth (mm)	Evapotranspiration (mm)	ET ^a (%)	ER (%)	T ^b (%)	T/ET (%)
S31 epikarst spring catchment	3282.2	1497.39	1784.81	54.38	3.16	51.22	94.19

^aET was evapotranspiration proportion in precipitation, calculated by $ET\% = (P - R)/P$

^bT was the proportion of transpiration to precipitation, estimated by $T = ET - E$

sources of groundwater supplies. Dispersed recharge consists mainly of local flow with percolation through fissures, whereas concentrated recharge primarily consists of surface runoff, which rapidly concentrates large volumes of water that flows into sinkholes (Chang et al. 2012). Karst aquifers have well-developed drainage systems with quick responses to rainfall (Fu et al. 2016; Deng et al. 2019). Groundwater recharge occurs due to precipitation, runoff, and recharge from surface water bodies (Mohamed et al. 2021). Previous groundwater recharge studies showed that the main recharge occurs in depressions (Chang et al. 2012). Tracer experiments revealed that 80% of the tracer in No.1 depression flowed out through S₃₁ spring with an arrival time from 3 h 32 min to 7 h 39 min, while 31% of the tracer in No.4 depression flowed out through the S₃₁ spring with an arrival time from 8 h 12 min to 11 h 22 min (Chang et al. 2012). However, this study only studies centralized recharge, not dispersed recharge.

In our study, the contributions of epikarst water recharge were 72.1% from summer precipitation and 27.9% from winter precipitation, which were in alignment with the timing of annual precipitation, ~80% of which occurred during the summer (Deng et al. 2020). Our studies also revealed that the renewal speed of epikarst water was rapid ~four months (Table 2). The surface was alternately covered with thin skeletal soils and exposed rock, which allows rainwater to recharge the karst aquifer quickly, leading to the faster speed conduit flow and the shorter MRT (Table 2). Furthermore, the MRT from throughfall to epikarst discharge (131 days) was a little longer than that from precipitation to epikarst discharge (121 days), which signified that the canopy interception prolonged the residency time of water within the system. The effects of fine-scale throughfall patterns on the generation of subsurface stormflow were minor (Hopp and McDonnell 2011). The groundwater hydrochemistry depends mainly on long-term water and rock interactions during water flow through fractures and conduits (Khan et al. 2019). Canopy interception should be given greater attention in the water management of forested karst catchments, because of uneven spatial and temporal rainfall distribution.

The above results are helpful for further study of hydrological processes and water resource control in the forested catchments of karst regions.

The difference in MRT results calculated by different isotopic methods may be related to not only isotope quality and isotope diffusion but also sampling method and study area. Our uniform sampling during the year is not only used to calculate MRT but also seasonal groundwater recharge and evaporation rate. The MRT method generally calculates the average residence time of slow flow without considering the influence of fast flow in karst area. So, to improve the accuracy of calculation MRT, it is suggested to take samples after the flood peak when the spring water is relatively stable. Because of this feature, this MRT method is also more applicable in the watershed with large watershed area, relatively sufficient water–rock interaction, and small spatial and temporal distribution difference of rainfall in the watershed.

Comparison of evaporation rates in forest catchments

Accurate and precise estimations of transpiration and evaporation rate are important. Two methods (direct and indirect) have been developed to quantify evaporation. Direct methods, such as field measurements using a lysimeter, provide high accuracy data of a small area (Kubota and Suzuki 1987; Zhao et al. 2015). However, extrapolating direct measurements of evaporation ratios for a small research site to a large area is difficult (Navneet and Jaywant, 2020). The indirect method estimates evaporation ratios by integrating a number of other measured data, such as rainfall, temperature, air pressure, gust velocity, and their correlations with evaporation, such as radiation, energy (Tajchman 1972), and water balances (Lane et al. 2004). However, these methods suffer from poor spatial representation, or are time-consuming and depend on the availability of data required to calibrate and validate the areal model (Navneet and Jaywant, 2020). In our studies, evaporation rates were first quantified by d-excess, and then transpiration ratios were calculated combining water balance methods. This methodology is useful for

Table 5 Evaporation ratios of the forest floor in previous studies

Source	Ratio (%)	Vegetation	Method
Stälfelt (1963)	20	Spruce	
Rutter (1966)	8	Red pine	
Baumgartner (1967)	10	Spruce	Energetic base radiation and energy balances
Tajchman (1972)	5	Spruce	
Hattori (1983)	8.9	Japanese cypress	
Kubota and Suzuki (1987)	3	Japanese cedar	micro lysimeter
Tamai and Hattori (1994)	18	Oak and azalea	
Tayoko Kubota and Yoshio Tsuboyama (2004)	4.9–5.5	mature forests	$\delta D/\delta^{18}O$
Liu wenjie et al. (2006)	4.6	tropical seasonal rain forest	$\delta D/\delta^{18}O$
Hu et al (2018)	7.1	Bare rock land	D-excess
	9.0	grassland	
	16.6	Shrub land	
	17.7	Cultivated land	
	21.4	Bare soil land	

quantifying groundwater budgets and groundwater resource assessment in karst area.

Previous research (in Table 5) has shown that the estimated ER (3.2%) using d-excess was similar to previous results for similar land cover (Tayoko and Yoshio 2004; Maki and Tadashi 1998; Liu et al. 2006), albeit lower than that of deciduous forests (8–10%) (Wilson et al. 2001), pine forests (8–16%) (Tayoko and Yoshio 2004), tropical eucalypt plantations (15–26%) (Lane et al. 2004), bare rocky land and bare soil land (7.1% and 21.4%, respectively) (Hu et al. 2018). The results from Hu et al. (2018) revealed that the evaporation rate of bare rocky land was lower than that of bare soil land, as precipitation can be quickly and directly recharged in the epikarst zone through fissures and conduits, resulting in little surface runoff. Chang et al. (2012) further confirmed that surface runoff accounted for only 0.63% of the total discharge of the catchment of the S₃₁ spring. The karst rock surface with large pore spaces and shallow soil greatly reduced the evaporation from the catchment. Furthermore, the dense and multi-layered canopies of subtropical forests effectively reduced evaporation from the forest floor (Tayoko and Yoshio 2004; Hu et al. 2018).

The transpiration proportion in evapotranspiration in the S₃₁ epikarst spring catchment was 51.22%, which suggested that the water flux from the vegetated catchment to atmosphere was primarily dominated by vegetation transpiration. In view of this advantage, vegetation transpiration should be paid more attention to in future management of groundwater in catchments. Plants with low water consumption were the first choice for the ecological restoration of rocky karst desertification. Furthermore, distinguishing evapotranspiration by transpiration and evaporation composition in catchments

was significant for researching the nitrogen and carbon cycle, due to the relationship between transpiration and carbon assimilation.

Conclusions

Groundwater recharge mainly originated from precipitation during the rainy season, which averaged 72% of the total annual rainfall. The MRT from throughfall to spring discharge (131 days) was a little longer than that from precipitation to spring discharge (121 days). The evaporation rates estimated by the d-excess method in a typical epikarst spring catchment were 3.16%. The d-excess method is more suited to calculate evaporation in hot and rainy areas. Our research provides a useful reference for the accurate estimation of transpiration rate and evaporation rates in future work.

Acknowledgements This work was funded by Key projects of Guangxi Natural Science Foundation (2022GXNSFDA035067) and the National Natural Science Foundation of China (41877206 and 42272298).

Data availability Use manuscript elements (Figures, Tables, and Methods) to help identify your data.

Declarations

Conflict of interest The authors declare no conflict of interest.

References

Ahmet Ş, İrfan Y, Ercan S (2020) Determination of recharge, storage and flow characteristics of a karst aquifer using multimethod approaches (Kocaeli, Turkey). *Hydrogeol J* 28:2141–2157

- Allen ST, Brooks JR, Keim RF et al (2014) The role of pre-event canopy storage in throughfall and stemflow by using isotopic tracers. *Ecohydrol* 7:858–868
- Baumgartner A (1967) Energetic base for differential vaporization from forest and agricultural lands. In: Sopper WE, Lull HW (eds) *Intern. Symp. For. Hydrol.* Pergamon, Oxford, pp 381–389
- Chang Y, Wu JC, Jiang GH et al (2012) The impact of overland flow on the variation of discharge and hydrochemistry of karst spring in peak cluster. *Shuili Xuebao* 43(9):1050–1057 (**In Chinese**)
- Clark ID, Fritz P (1997) *Environmental isotopes in hydrogeology.* Lewis, Boca Ration
- Dansgaard W (1964) Stable isotopes in precipitation. *Tellus* 16:436–468
- Deng Y, Jiang ZC, Kuo YM et al (2019) Effects of canopy interception on epikarst water chemistry and its response to precipitation in Southwest China. *Carbonates Evaporites* 34:273–282
- Deng Y, Ke J, Wu S et al (2020) Responses of plant water uptake to groundwater depth in limestone outcrops. *J Hydrol* 590:125377
- Ford DC, Williams PW (2007) *Karst hydrogeology and geomorphology.* Wiley, Chichester
- Fu TG, Chen HS, Wang KL (2016) Structure and water storage capacity of a small karst aquifer based on stream discharge in southwest China. *J Hydrol* 534:50–62
- Gat JR (1996) Oxygen and hydrogen isotopes in the hydrologic cycle. *Annu Rev Earth Planet Sci* 24:225–262
- Gholam HK, Rahim B, Fahimeh R (2016) Determining the groundwater potential recharge zone and karst springs catchment area: Saldoran region, western Iran. *Hydrogeol J* 24:1981–1992
- Hartmann A, Goldscheider N, Wagener T et al (2014) Karst water resources in a changing world: Review of hydrological modeling approaches. *Rev Geophys* 52(3):218–242
- Hattori S (1983) The seasonal variation of evaporation from the forest floor in a hinoki stand. *J Jpn for Soc* 65:9–16 (**In Japanese**)
- Hiroaki K, Yuichi O, Kazuki N et al (2013) Effect of canopy interception on spatial variability and isotopic composition of throughfall in Japanese cypress plantations. *J Hydrol* 504:1–11
- Hopp L, McDonnell JJ (2011) Examining the role of throughfall patterns on subsurface stormflow generation. *J Hydrol* 409:460–471
- Hu YD, Liu ZH, Zhao M et al (2018) Using deuterium excess, precipitation and runoff data to determine evaporation and transpiration: a case study from the Shawan Test Site, Puding, Guizhou, China. *Geochim Cosmochim Acta* 242:21–33
- Huang TM, Pang ZH (2012) The role of deuterium excess in determining the water salinization mechanism: a case study of the arid Tarim River Basin, NW China. *Appl Geochem* 27:2382–2388
- Jiang GH, Zhang Q (2011) Change of dissolved inorganic carbon (DIC) in karst peak cluster during natural restoration: a case study in Yaji station. *Carsologica Sinica* 30(4):397–402 (**In Chinese**)
- Khan Q, Kalbus E, Alshamsi DM et al (2019) Hydrochemical analysis of groundwater in Remah and Al Khatim regions. *United Arab Emir Hydrol* 6(3):60
- Kubota J, Suzuki M (1987) Studies on soil water movement in the Paleozoic to Mesozoic area. 1. Measurement of evaporation from forest floor using microlysimeters. *Proc Jpn for Soc* 98:555–558 (**In Japanese**)
- Lane PN, Morris J, Zhang NN (2004) Water balance of tropical eucalypt plantations in Southeastern China. *Agric for Meteorol* 124:253–267
- Lee KS, Kim Y (2007) Determining the seasonality of groundwater recharge using water isotopes: a case study from the upper North Han River basin. *Korea Environ Geol* 52(5):853–859
- Liu WJ, Li PJ, Li HM et al (2006) Estimation of evaporation rate from soil surface using stable isotopic composition of throughfall and stream water in a tropical seasonal rain forest of Xishuangbanna, Southwest China *Acta Ecologica Sinica* 26(5):1303–1310
- Maki T, Tadashi T (1998) Evaluation of evaporation rate from forested soil surface using stable isotopic composition of soil water in a headwater basin. *Hydrol Process* 12:2093–2103
- Maloszewski P, Stichler W, Zuber A, Rank D (2002) Identifying the flow system in a karstic-fissured-porous aquifer, Schneelpe, Austria, by modeling of environmental ^{18}O and ^3H isotopes. *J Hydrol* 256:48–59
- Martin M, Miroslav T, Vojtech V et al (2020) Past (1971–2018) and future (2021–2100) pan evaporation rates in the Czech Republic. *J Hydrol* 590:125390
- Mauro M, Daniele Z, Barbara S et al (2020) Spatial distribution and interannual trends of $\delta^{18}\text{O}$, $\delta^2\text{H}$, and deuterium excess in precipitation across North-Eastern Italy. *J Hydrol* 598:125749
- Mohamed MM, Parimalarenganayaki S et al (2021) Review on the use of environmental isotopes for groundwater recharge and evaporation studies in the GCC countries. *Groundw Sustain Dev* 12:100546
- Navneet K, Jaywant HA (2020) A fast method to measure the evaporation rate. *J Hydrol* 594:125642
- Reddy MM, Schuster P, Kendall C et al (2006) Characterization of surface and ground water $\delta^{18}\text{O}$ seasonal variation and its use for estimating groundwater residence times. *Hydrol Process* 20:1753–1772
- Rusjan S, Sapač K, Petrič M et al (2019) Identifying the hydrological behavior of a complex karst system using stable isotopes. *J Hydrol* 577:123956
- Rutter AJ (1966) Studies on the water relations of pinus sylvestris in plantation conditions IV. Direct observations on the rates of transpiration, evaporation of intercepted water, and evaporation from the soil surface. *J Appl Ecol* 3:393–405
- Stalfelt MG (1963) On the distribution of the precipitation in a pruned stand. In: Rutter AJ, Whitehead FH (Eds). Blackwell, Oxford. pp. 115–126.
- Tajchman SJ (1972) The radiation and energy balances of coniferous and deciduous forests. *J Appl Ecol* 9:359–375
- Tamai K, Hattori S (1994) Modeling of evaporation from a forest floor in a deciduous broad leaved forest and its application to a basin. *J Jpn for Soc* 76:233–241 (**In Japanese**)
- Tayoko KY (2004) Estimation of evaporation rate from the forest floor using oxygen-18 and deuterium compositions of throughfall and stream water during a non-storm runoff period. *J Res* 9:51–59
- Wilson KB, Hanson PJ, Mulholland PJ (2001) A comparison of methods for determining forest evapotranspiration and its components: sap-flow, soil water budget, eddy covariance and catchment water balance. *Agric for Meteorol* 106:153–168
- Zhao P, Li S, Li F et al (2015) Comparison of dual crop coefficient method and Shuttleworth-Wallace model in evapotranspiration partitioning in a vineyard of northwest China. *Agric Water Manage* 160:41–56
- Zhu XY, Zhang ML, Wu X et al (2017) The relationship between $\delta^{18}\text{O}$ characteristics of the precipitation (heavy rainfall or rainstorm) and its water vapor sources in Guilin. *China Carsologica Sinica* 36(2):139–161 (**In Chinese**)

Publisher's Note Springer Nature remains neutral with regard to jurisdictional claims in published maps and institutional affiliations.

Springer Nature or its licensor (e.g. a society or other partner) holds exclusive rights to this article under a publishing agreement with the author(s) or other rightsholder(s); author self-archiving of the accepted manuscript version of this article is solely governed by the terms of such publishing agreement and applicable law.